Supporting information

Supporting notes

The simulation setup and the material properties employed in our numerical analysis, aimed at comparing with the experimental results reported in prior work, are detailed in Fig. S1. Fig. S1a depicts the simulation setup, while the permittivity and permeability values for Carbon black/PLA are derived from previous research.[25] Notably, since the measured permittivity and permeability data were only available for the 8.2 – 12.4 GHz range, we applied a linear approximation to extend these properties to the 4-18 GHz range. This extension was based on the observed linear trend in the measured properties.

$$Re(\varepsilon) = (Frequency(in\ GHz) - 8.2) \times (-0.9457) + 17.73$$

$$Im(\varepsilon) = (Frequency(in\ GHz) - 8.2) \times (-1.4070) + 24.71$$

Our simulation model setup was then validated by correlating our results with the experimental findings[25] for both single-layered structures with diameters of 1.2 mm and 1.6 mm (as shown in Fig. S1 (c)) and for three-layered octet-truss structures (Fig. S1 (d)). Although conducting experiments is beyond the scope of this study, we demonstrated the feasibility of fabricating the proposed octet-truss and octet-foam structures. This was accomplished using fused filament fabrication (FFF) 3D printing to create three-layered structures of octet-truss and octet-foam, as depicted in Fig. S1 (e) and (f).

Fig. S2 examines the relationship between material thickness and its impact on absorption, reflection, and transmission responses in a material with 100% infill, referred to as a solid material. We investigated the electromagnetic wave response across a range of thicknesses, incrementally increasing from 0.2 mm to 10 mm in 0.2 mm steps (encompassing 50 different thicknesses) within the 4 – 18 GHz frequency range. A notable observation is the sharp decline in transmission with increasing thickness; for instance, transmission dropped from 62.3% at 0.2 mm to just 7.50% at 2.0 mm at 4 GHz. While absorption generally increased as thickness grew, owing to reduced transmission and the material's inherent dielectric loss, it eventually reached a plateau. This plateau is attributed to the reflection caused by the impedance mismatch with the complex permittivity of free space. An example of this is the absorption rate at 4 GHz, which was 44.7% for a thickness of 6.0 mm, nearly identical to the 43.4% absorption rate at a thickness of 10.0 mm. These findings highlight the limitations of relying on the material alone, without incorporating structural absorption features.

Supporting figures

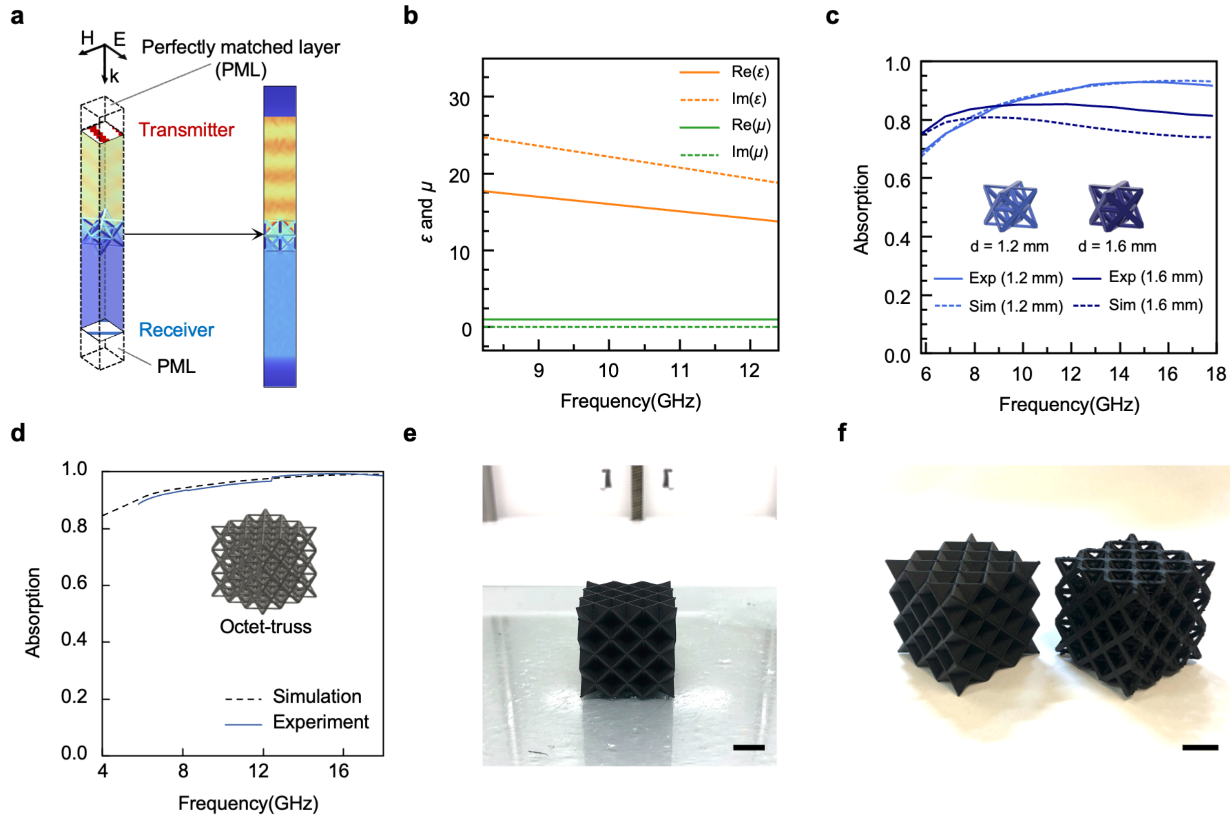

Fig. S1. Configuration and validation of simulations through comparison with experimental data. (a) Illustration of the simulation setup, where the EM wave absorbing structure is positioned in the middle, while the transmitter and receiver are situated at the end. (b) Real and imaginary values of permittivity (ε) and permeability (μ) of carbon black-polylactic acid (CB-PLA) material. (c) Comparison between the simulations conducted in this study's setup and experimental results from prior research[25] focusing on octet-truss structures featuring strut diameters of 1.2 mm and 1.6 mm, with a cell length of 10 mm. (d) Contrasting simulation and experimental outcomes on the electromagnetic wave absorption in a three-layer of octet-truss with 10 mm unit cell length. (e) 3D-printed octet-foam structure demonstrating its manufacturability (f) 3D-printed models: octet-foam (on the left) and octet-truss (on the right), each featuring unit cell length of 10 mm and a sheet thickness and strut diameter of 1.6 mm. Scale bars, 10 mm (e,f)

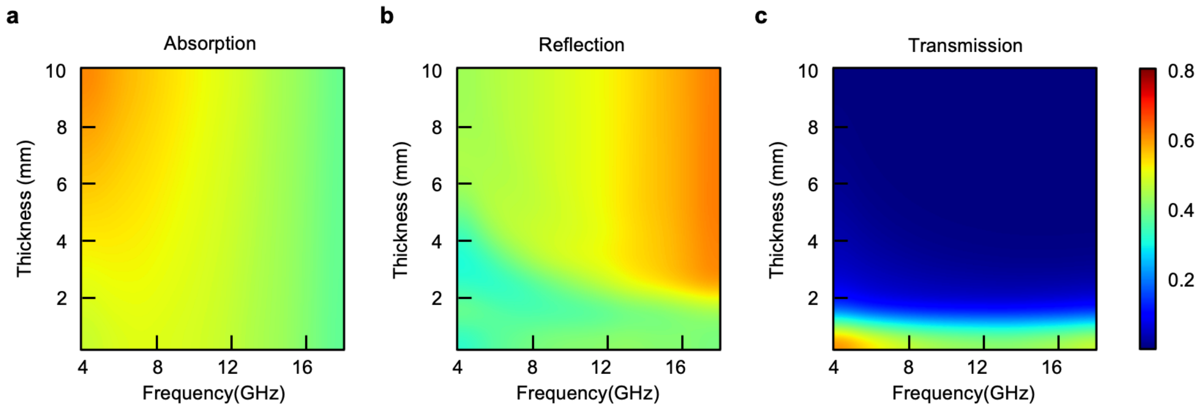

Fig. S2. Electromagnetic wave response of solid material (100% infill of carbon black-polylactic acid) with varied thickness ranging from 0.2 mm to 10 mm. (a) Absorption, (b) reflection, and (c) transmission.

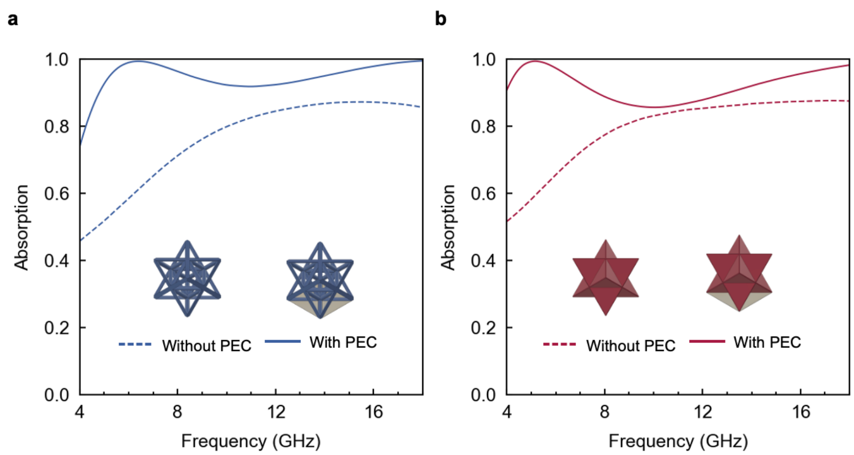

Fig. S3. Effect of perfect electric conductor to the electromagnetic wave absorption in (a) octet-truss and (b) octet-foam.

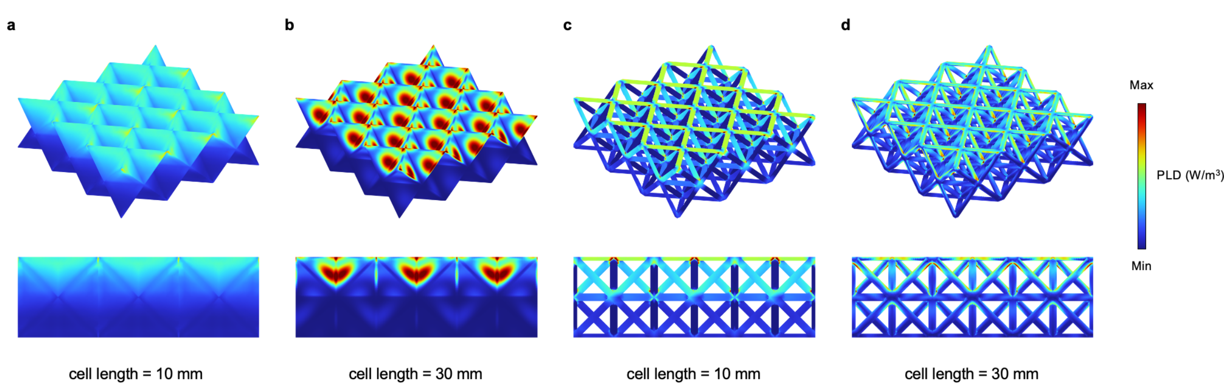

Fig. S4. Distribution of power loss density at 15 GHz for (a) octet-foam with 10 mm cell length, (b) octet-foam with 30 mm cell length, (c) octet-truss with 10 mm cell length and (d) octet-truss with 30 mm cell length.

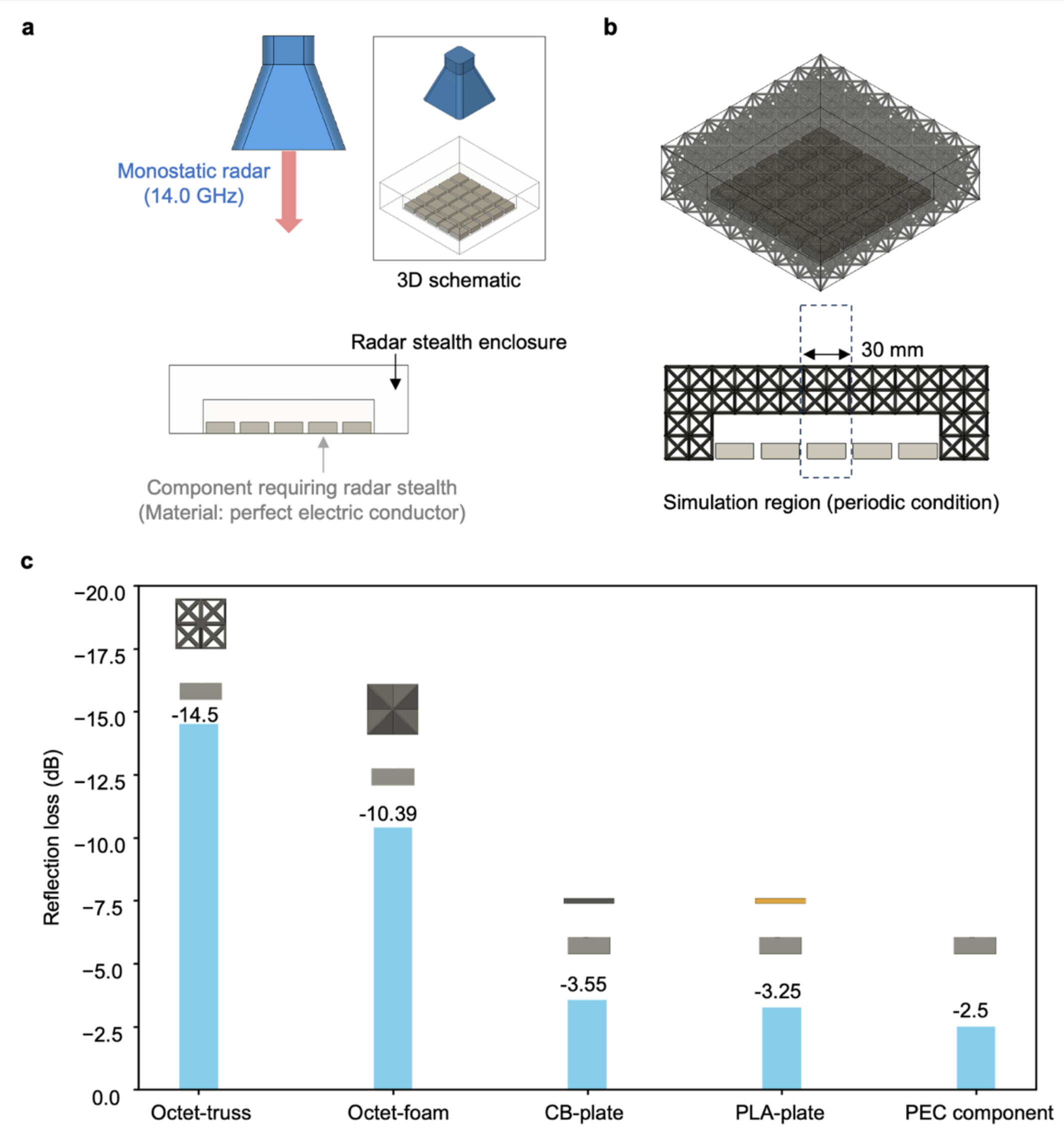

Fig. S5. Reflective loss comparison in stealth enclosure applications. (a) Illustration of a monostatic radar emitting 14 GHz electromagnetic wave towards a component made of perfect electric conductor (PEC). (b) A 30 mm octet-truss used as a stealth enclosure design example. (c) Comparative reflection loss data for a 30 mm octet-truss, a 30 mm octet-foam, a CB/PLA plate with 3 mm thickness, a PLA plate with 3 mm thickness, and an unenclosed bare PEC component.

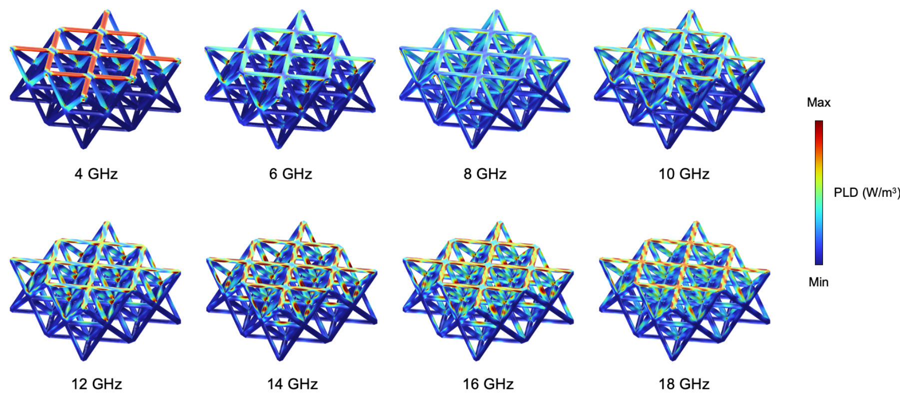

Fig. S6. Power loss density plot of octet-truss with 50 mm cell length across frequencies ranging from 4 GHz to 18 GHz, demonstrating different locations of power loss concentration resulting from the varying interferences.

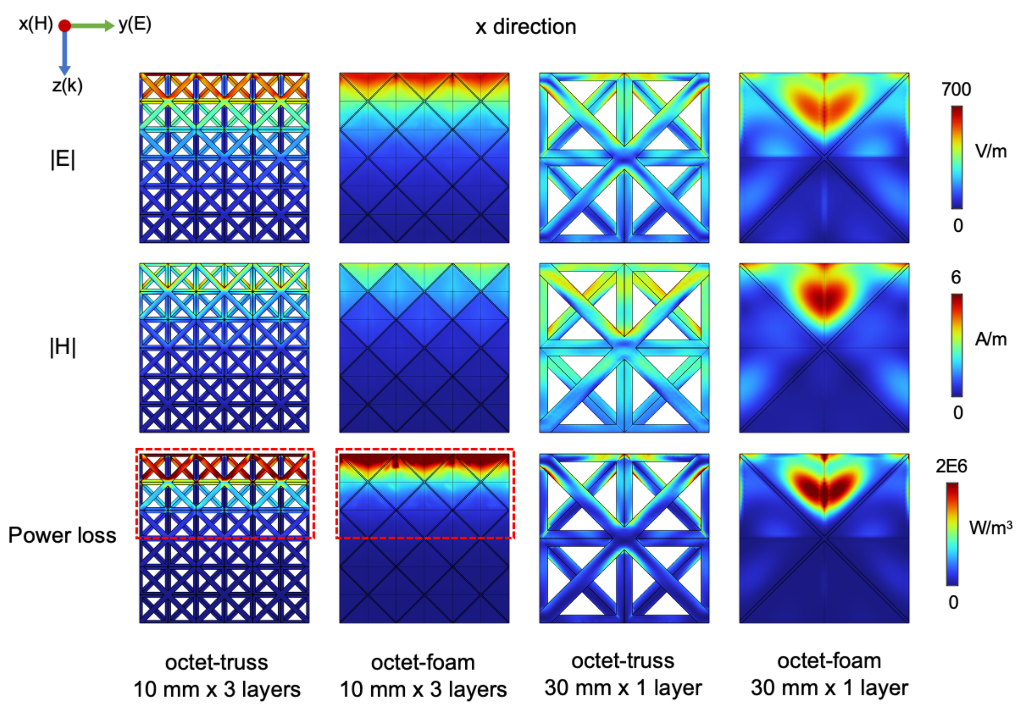

Fig. S7. Side view of 3D plots showcasing electric field, magnetic field, and power loss density within octet-truss and octet-foam structures. The comparison contrasts the configuration with multiple layers (comprising three layers with a 10 mm cell length) against the single-layer arrangement (a single layer with a 30 mm cell length) at 15 GHz.

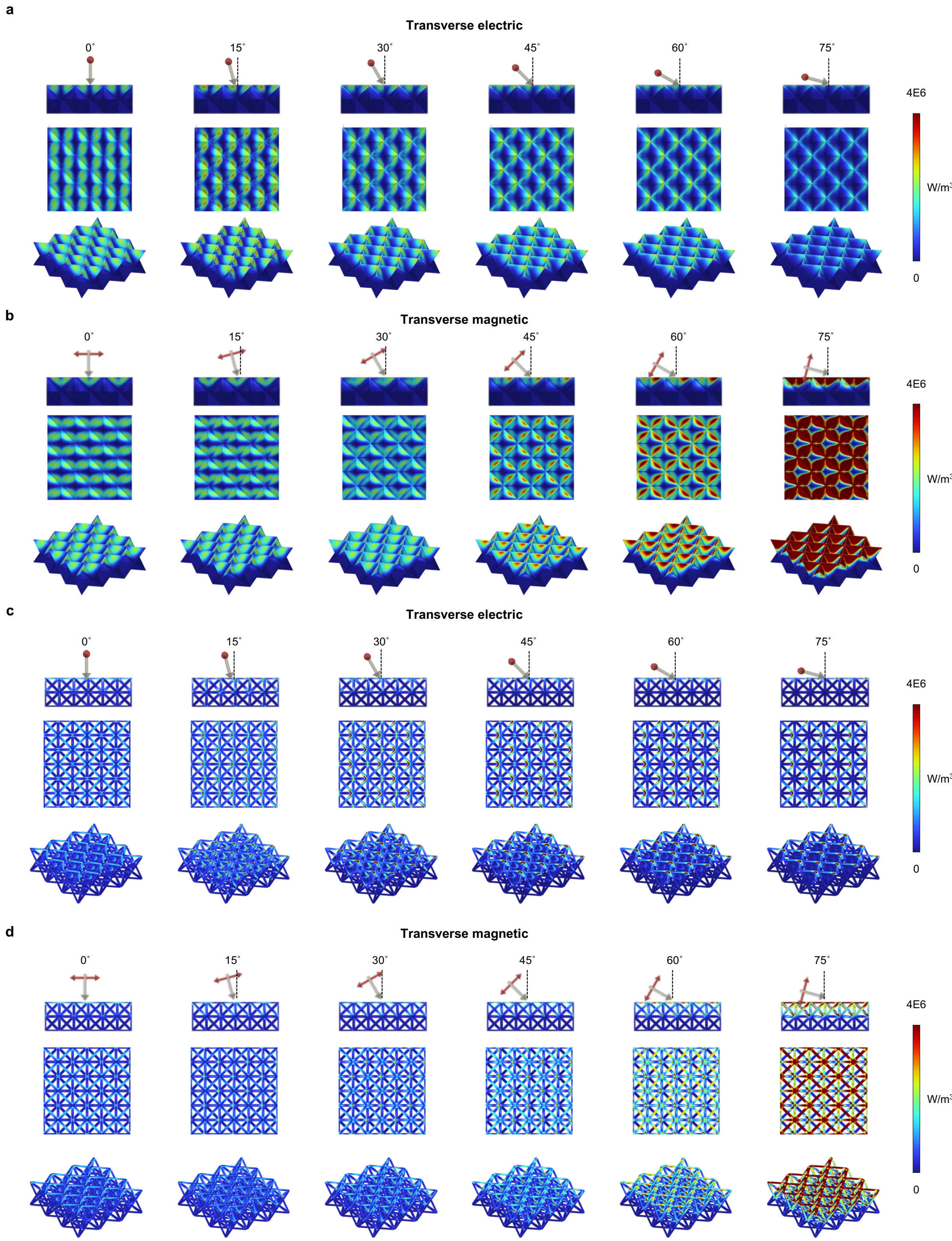

Fig. S8. Power loss density plot at 12 GHz of (a), (b) octet-foam and (c), (d) octet-truss when subjected to transverse electric and transverse magnetic polarization, exhibiting fluctuations in power loss concentration as the incident angle is altered within the range of 0° to 75°

Supporting tables

Table. S1. Comparative analysis of the low density and load-bearing unit cell structured broadband electromagnetic wave absorber.

Reference	**Unit cell**	**Geometrical parameters (number of variables)**	**Target bandwidth (Reflection loss < -10dB)**	**Fabrication methods**
[11]	Honeycomb	Fixed unit cell structure (1)	2 – 18 GHz	Dipping premade honeycomb core
[12]	Honeycomb	Depth (4), wall thickness (4), cell length (3)	5.8 – 18 GHz	Resin impregnation, layer stacking, and autoclave
[13]	Honeycomb	Thickness (3)	2 – 18 GHz	Stagger stacking, binding, and expanding paper-based composites honeycomb core
[14]	Honeycomb	Side length (3), height (3)	2.5 – 8 GHz	Dipping paper honeycomb with carbon black with plaster poured into the structure
[15]	Honeycomb	Layer (2)	4 – 18 GHz	Vacuum encapsulation of carbon black coated honeycomb core
[16]	Honeycomb	Length (3) × depth (4) (total 12)	3 – 16 GHz	Molding glass/epoxy-MWCNT prepreg and vacuum bagging stacked layers
[17]	Honeycomb	Fixed unit cell structure (1)	3.53 – 24 GHz	Attaching resistive patch to 3D printed honeycomb skeleton
[24]	Gyroid	sheet-strut composition (2) × Volume fraction (4) (total 8) + Cell size (4),	2 – 40 GHz	Dipping 3D printed ABS to carbon-based composition
[25]	Octet-truss	Volume fraction (3), layers (4), length (4)	4 – 18 GHz	3D printing carbon-black/PLA
[26]	Kelvin-foam	Volume fraction (4), Length (5)	4 – 18 GHz	3D printing carbon-black/PLA
This work	Octet-truss, octet-foam	Sheet-strut composition (2) × Unit cell length (4) (total 8), solid/effective medium (11), layers (2), volume fraction (4)	4 – 18 GHz	Numerical analysis based on validated 3D printing process (same as reference 24,25,26)